

Pressure study of quantum criticality in CeCoIn₅

F. Ronning,¹ C. Capan,^{1,*} E. D. Bauer,¹ J. D. Thompson,¹ J. L. Sarrao,¹ and R. Movshovich¹

¹Los Alamos National Laboratory, Los Alamos, New Mexico 87545, USA

(Received 15 November 2005; published 28 February 2006)

We report resistivity measurements in the normal state of CeCoIn₅ down to 40 mK and simultaneously in magnetic fields up to 9 T in the [001] crystallographic direction and under pressures up to 1.3 GPa. At ambient pressure the data are consistent with a field tuned quantum critical point coincident with the superconducting upper critical field H_{c2} , as observed previously. We find that with increasing pressure the quantum critical point moves inside the superconducting dome to lower fields. Thus, we can rule out that superconductivity is directly responsible for the non-Fermi-liquid behavior in CeCoIn₅. Instead, the data point toward an antiferromagnetic quantum critical point scenario.

DOI: [10.1103/PhysRevB.73.064519](https://doi.org/10.1103/PhysRevB.73.064519)

PACS number(s): 74.70.Tx, 71.27.+a, 72.15.Eb, 75.40.Cx

A quantum critical point is simply the point at which a second-order phase transition occurs at $T=0$, where quantum fluctuations are present. Classical phase transitions are now well understood. While theoretically there is a natural extension to $T=0$,¹⁻³ the experimental systems (and in particular heavy-fermion systems) display serious discrepancies with these predictions.⁴ As disorder may profoundly influence the behavior at a quantum critical point, there is great benefit in examining quantum critical systems which are stoichiometric, and hence, relatively disorder free. CeCoIn₅ is one of a relatively small number of such systems.

CeCoIn₅ is a heavy-fermion superconductor with $T_c = 2.3$ K.⁵ The normal-state possesses non-Fermi-liquid properties in zero field [T linear resistivity, $T \ln(T)$ specific heat, and modified Curie-Weiss χ , compared to the Fermi-liquid expectations of T^2 resistivity, T linear specific heat, and constant χ] indicative of a nearby underlying quantum critical point.^{6,7} By applying the magnetic field along the tetragonal c axis a field-tuned quantum critical point (QCP) was identified at $H_{\text{QCP}} = 5$ T.^{8,9} The fact that the superconducting upper critical field H_{c2} is also at 5 T raises the question of whether superconducting fluctuations could be responsible for the field-tuned non-Fermi-liquid behavior. However, this observation (that $H_{c2} \approx H_{\text{QCP}}$) is likely to be an accidental coincidence for several reasons: (i) it is not clear if a superconductor has sufficiently strong fluctuations to produce an extended critical regime, (ii) the superconducting transition itself becomes first order below 0.7 K in CeCoIn₅,¹⁰ which should cutoff any diverging fluctuations, and (iii) similarities in the zero-field pressure-temperature phase diagrams of CeRhIn₅ and CeCoIn₅ suggests that CeCoIn₅ at ambient pressure is in close proximity to an antiferromagnetic quantum critical point, as is observed in CeRhIn₅.⁷ However, two experiments designed to separate H_{QCP} from H_{c2} , via magnetic field anisotropy¹¹ or Sn-doping studies,¹² failed to do so. Applying the magnetic field in the ab plane increases H_{c2} to 12 T, while in Sn doping studies the c axis H_{c2} was suppressed to as low as 2.75 T for CeCoIn_{4.88}Sn_{0.12}. Despite this variation in H_{c2} by more than a factor of 4, one did not observe the appearance of an additional ordered phase above H_{c2} , nor a Fermi-liquid regime at the superconducting upper critical field, with either specific heat or resistivity measurements. This suggests that the two critical fields are inherently linked together.

The pressure phase diagram of CeRhIn₅ alluded to above suggests that pressure may be an effective means of suppressing criticality in CeCoIn₅ if an antiferromagnetic QCP is indeed still the origin of the non-Fermi-liquid behavior in both systems. This is supported by measurements of resistivity in zero field,⁷ specific heat,¹³ and NQR (Ref. 14) which appear to restore Fermi-liquid behavior with increasing pressure in CeCoIn₅. In addition, de Haas-van Alphen (dHvA) results at high fields show the effective mass of the two-dimensional (2D) cylindrical β sheet (which increases as H_{c2} is approached from above) decreases with increasing pressure.¹⁵ The evolution of the field-tuned QCP with pressure is best identified by performing measurements with magnetic field. This is precisely how H_{QCP} was originally identified to be close to H_{c2} at ambient pressure.^{8,9} In this paper we report resistivity measurements of CeCoIn₅ under pressure with magnetic field up to 9 T applied along the c axis and temperatures down to 40 mK. We find that the QCP is strongly suppressed inside the superconducting dome and hence is no longer coincident with H_{c2} as pressure is increased. This gives compelling evidence that the origin of the non-Fermi-liquid behavior is not associated with superconductivity, but rather related to an order competing with superconductivity, most likely antiferromagnetism.

Resistivity under pressure was obtained by a four point measurement in a Cu-Be piston cell attached to the temperature regulation stage on a dilution refrigerator. The use of silicone as the pressure transmitting medium ensures hydrostatic pressure ($\Delta P \sim 0.01$ GPa). A single crystal, aligned to within 5° of the c axis, was measured in fields up to 9 T. Field sweeps at 100 mK identified H_{c2} as 4.95, 4.95, 4.63, and 4.0 T at the four measured pressures of 0, 0.05, 0.6, and 1.3 GPa. The pressure was determined independently by measuring the superconducting transition of a Sn sample by ac susceptibility.

At ambient pressure the quantum critical field was determined by tracking the divergence of the T^2 coefficient of resistivity in the ever shrinking window of the Fermi-liquid regime.⁸ We follow the same recipe here for four different pressures 0, 0.05, 0.6, and 1.3 GPa. The raw resistivity data is shown versus T^2 in Fig. 1. Panels (a) through (d) show data for various fields at a given pressure, while panels (e) and (f) present resistivity curves for various pressures at constant magnetic field. Recall that in the Fermi-liquid regime

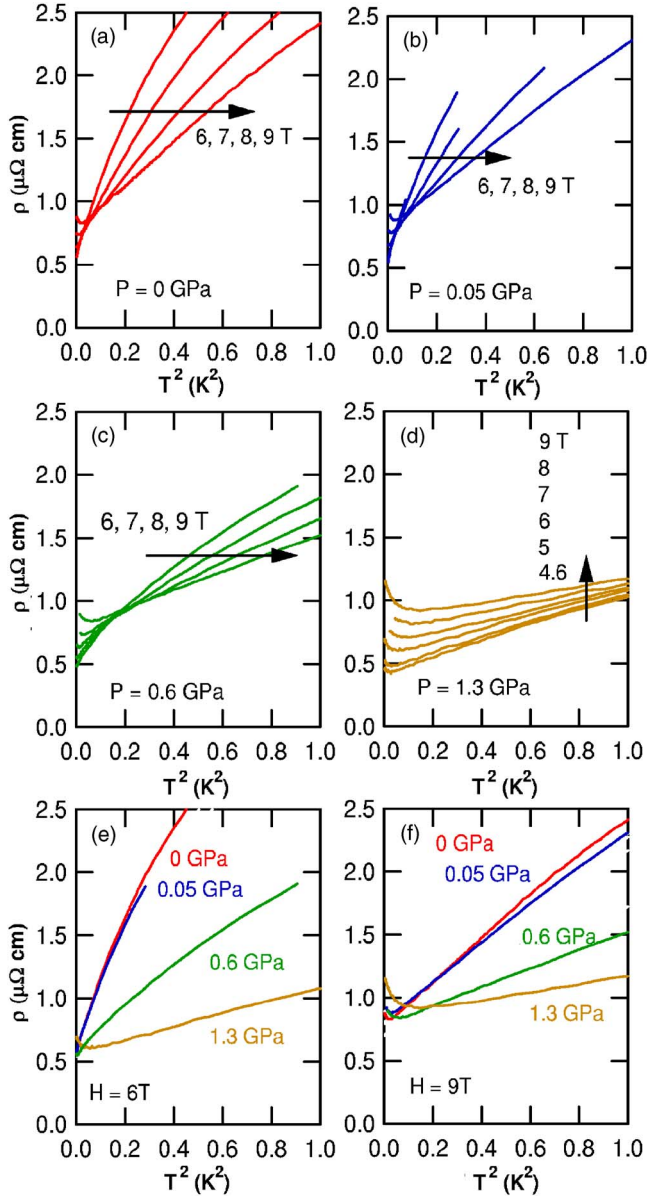


FIG. 1. (Color online) Resistivity of CeCoIn₅ for $H\parallel c$ axis and current in the ab plane plotted versus T^2 to highlight the Fermi liquid regime for fields above the superconducting upper critical field. $H_{c2}=4.95, 4.95, 4.63,$ and 4.0 T for $P=0, 0.05, 0.6,$ and 1.3 GPa, respectively. Panels (a) through (d) are taken at the constant pressure indicated, and panels (e) and (f) are four different pressures measured at the same value of the magnetic field indicated in the plot.

$\rho = \rho_0 + AT^2$. Thus, a straight line in Fig. 1 would correspond to a well established Fermi-liquid behavior whose slope is proportional to the square of the effective mass. At high fields [e.g., 9 T; see Fig. 1(f)] the Fermi-liquid regime extends over a wide temperature range. At low temperatures there is an upturn in the data, which is believed to originate from quasiparticles reaching the $\omega_c\tau \approx 1$ limit, and hence this is also a feature of the Fermi-liquid regime in CeCoIn₅.⁸ We note that a similar observation was made in a very clean UPt₃ crystal.¹⁶ For the purpose of analysis, this prevents us from fitting $\rho = \rho_0 + AT^2$ down to the lowest temperature mea-

sured; rather, we fit over a range which maximizes the A coefficient. As the magnetic field is reduced toward H_{c2} the temperature range of the T^2 Fermi-liquid regime decreases monotonically.

There are several features evident in the raw data which we will attempt to quantify below. Beginning with the ambient pressure data in Fig. 1(a), there is a dramatic increase in the inelastic scattering as the magnetic field is lowered. Simultaneously, the A coefficient grows, and the Fermi-liquid regime becomes vanishingly small. Let us contrast this with the 1.3 GPa data in Fig. 1(d). While the A coefficient also increases with decreasing field the effect is not nearly as dramatic as at ambient pressure. Furthermore, there is still a well established Fermi liquid at 4.6 T (which is just above $H_{c2}=4$ T) on a temperature range significantly larger than at 6 T for ambient pressure. This is shown both by a large linear regime on the plot of ρ versus T^2 and by the upturn still present at the lowest measured temperatures. As for the resistivity data for 0.05 and 0.6 GPa, we find it displays a smooth evolution between the ambient pressure and 1.3 GPa extremes we just discussed. We also should note that as the pressure increases the A coefficient is also rapidly suppressed as can be seen in Figs. 1(e) and 1(f).

To quantify the above behavior in the Fermi-liquid regime, we plot the A coefficient versus field in Fig. 2(a) for each measured pressure. The divergence of the A coefficient, and hence the effective mass, is clearly suppressed with increasing pressure. Since pressure is known to increase the Kondo temperature in Ce Kondo lattice systems, we need to be certain that the reduction of A is not solely a decrease of the overall scale. For that purpose, we parametrize the divergence of A with the form $A = A_0(H - H_{QCP})^\alpha$ with A_0 and H_{QCP} as adjustable parameters. This form was used by Paglione *et al.* to identify the critical field as $H_{QCP} = 5.1$ T with $\alpha = -1.37$.⁸ By keeping α fixed at -1.37 we find both A_0 and H_{QCP} to decrease with increasing pressure. The values of A_0 are 14.1, 15.9, 12.0, and 8.2 $\mu\Omega \text{ cm}/\text{K}^2$ for 0, 0.05, 0.6, and 1.3 GPa, respectively. The behavior of A_0 can be understood from the general view of increasing the Kondo temperature and stabilizing the Fermi liquid with increasing pressure, as commonly observed in Ce compounds.¹⁷ We attribute the decreasing H_{QCP} to the fact that the critical field is moving inside the superconducting dome. The latter point is emphasized in Fig. 2(b). The critical fields from the fits above are plotted together with H_{c2} . The fact that the critical field moves inside the superconducting dome implies that we do not have a superconducting critical point. It is interesting to note that the pressure at which the extrapolated critical field reaches 0 T (~ 1.1 GPa) is close to the pressure at which the superconducting transition temperature is maximum (~ 1.3 GPa), a common feature of a wide variety of quantum critical systems.¹⁸

Finally, we extend our analysis of the data beyond the Fermi-liquid regime. Figure 3 presents an image plot of $\partial \ln(\rho - \rho_0) / \partial \ln(T)$ in the H - T plane for $P=0$ and $P=1.3$ GPa. Similar plots have been made for YbRh₂Si₂ (Ref. 19) and Sr₃Ru₂O₇ (Ref. 20) to help identify the critical field. The logarithmic derivative gives the value of the exponent n assuming the resistivity has the form $\rho = \rho_0 + AT^n$. The low-temperature regime of the resistivity upturn has been sup-

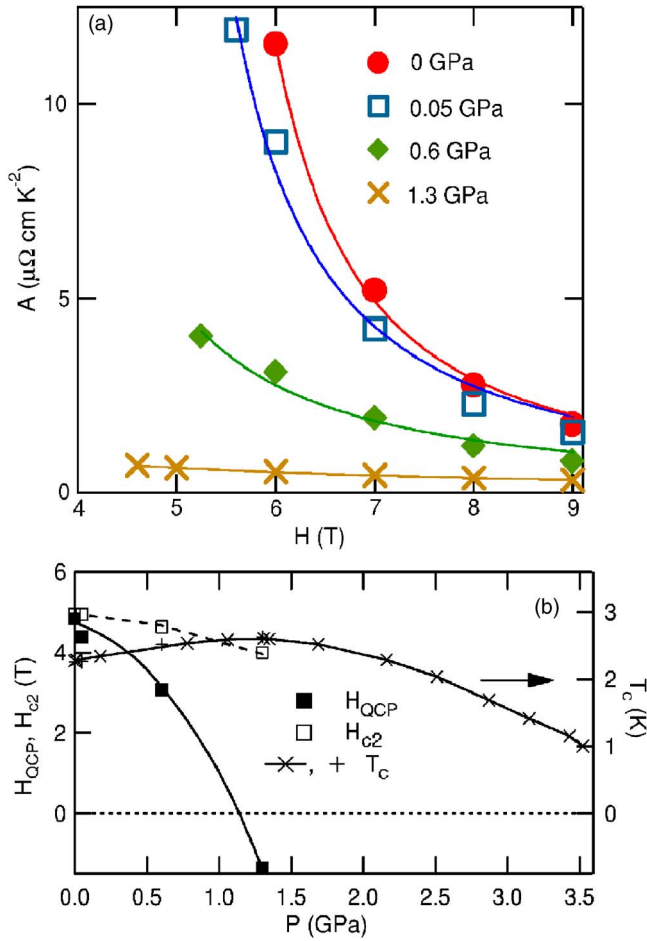


FIG. 2. (Color online) (a) The T^2 coefficient of the resistivity extracted from the data presented in Fig. 1. The solid lines are fits to $A=A_0(H-H_{\text{QCP}})^{-1.37}$. The values of H_{QCP} from the fits are plotted in (b) along with the values of the superconducting upper critical field and the superconducting T_c in zero field versus pressure. The \times 's are obtained from Ref. 7. Lines in (b) are guides to the eye.

pressed, as the form of ρ is inappropriate in this regime. While for $P=0$ the data again suggests that the quantum critical field occurs at the superconducting upper critical field of 5 T, it does not seem possible to make a similar statement for the $P=1.3$ GPa data. The open symbols mark the temperature where the Fermi liquid fits deviate by more than 2% from the data. This quantity should go to zero at the quantum critical point. At ambient pressure we see that this Fermi crossover temperature is rapidly vanishing as H_{c2} is approached. At 1.3 GPa a linear extrapolation yields a quantum critical point of 0.5 T, which is well inside the superconducting upper critical field of 4 T, and in reasonable agreement with our fit of the A coefficient versus magnetic field.

Thus, by applying hydrostatic pressure we have now successfully separated the critical field from the superconducting upper critical field, and we conclude that it was merely an accidental coincidence that $H_{\text{QCP}}=H_{c2}$ at ambient pressure for magnetic field along the c axis.^{8,9} Note that by adding an additional tuning parameter, namely, pressure, the field tuned critical point near H_{c2} , now becomes a line of critical points in the H - P plane. A consequence of this is that, while ambi-

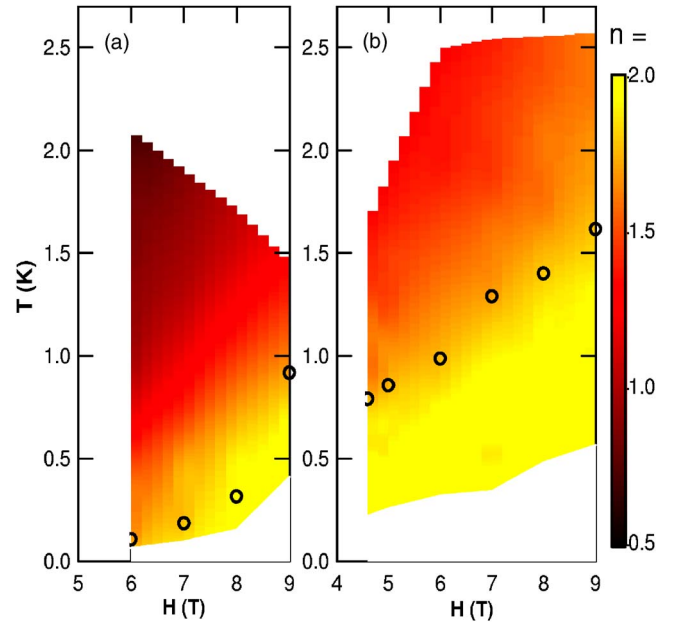


FIG. 3. (Color online) An image plot of $\partial \ln(\rho-\rho_0)/\partial \ln(T)$ for (a) ambient pressure and (b) 1.3 GPa. The open circles represent the Fermi crossover temperature as discussed in the text.

ent pressure CeCoIn₅ possesses a field tuned QCP, pressure tuning at zero field should find a critical pressure which can be accessed with positive pressure. It is hoped that measurements within the vortex cores will provide more direct evidence of this.

One can next speculate as to the true origin of the quantum critical fluctuations which produce the non-Fermi-liquid behavior in CeCoIn₅. From the initial comparison of the CeRhIn₅ and CeCoIn₅ phase diagrams under pressure, it has been suggested that the origin of the non-Fermi-liquid behavior is the presence of an antiferromagnetic quantum critical point.⁷ This speculation has been supported indirectly by numerous means. Since one expects both magnetic field and pressure to suppress antiferromagnetism in this compound, the fact that we observe the quantum critical point to rapidly move within the superconducting dome with increasing pressure is also consistent with this picture. Recently, dHvA results on CeRhIn₅ under pressure show that there is a quantum critical pressure of 2.35 GPa at which the Fermi surface undergoes a local to itinerant crossover of the $4f$ electrons.²¹ Given that the high-pressure dHvA frequencies agree well with those observed in CeCoIn₅ at ambient pressure, it is tempting to suggest that CeCoIn₅ at ambient pressure lies slightly above this high-field critical pressure.

While this provides a consistent perspective, there are still several unresolved issues. There is no explanation for why Sn doping was unable to separate the quantum critical point from the superconducting upper critical field over such a wide range in doping.¹² It is possible that Sn doping creates a very extended non-Fermi-liquid regime.²² Furthermore, if at ambient pressure in CeCoIn₅ the critical field of 5 T refers to a field suppression of an antiferromagnetic state, one must ask the question as to why the magnetic transition has not been observed at smaller fields? Perhaps this is tied to a

typically overlooked point that it is difficult to unify the non-Fermi-liquid behavior at zero field with the slightly different non-Fermi-liquid properties observed at H_{c2} , and it is possible that multiple critical points must be invoked to explain all the features of CeCoIn₅.²³ Our results also raise several questions in the related compound, CeRhIn₅. It is necessary to confirm in CeRhIn₅ that the critical pressure identified by dHvA (Ref. 21) does indeed correspond to an antiferromagnetic quantum critical point. We would also like to know if CeRhIn₅ has a similar line of critical points in the H - P plane as identified here. We hope that future measurements can resolve these issues.

In conclusion, we have studied resistivity of CeCoIn₅ un-

der pressure and in high magnetic fields. We demonstrate that the quantum critical field moves inside the superconducting dome with increasing pressure, which rules out a novel superconducting quantum critical point. This further suggests that the quantum critical behavior is most likely associated with an as yet undetected antiferromagnetic quantum critical point.

We would like to thank V. Sidorov and T. Park for helpful discussions, the T_c versus P data shown in Fig. 2(b), and assistance with the pressure cell. Work at Los Alamos National Laboratory was performed under the auspices of the U.S. Department of Energy.

*Present address: Department of Physics, Louisiana State University, Baton Rouge, LA 70803.

¹J. A. Hertz, Phys. Rev. B **14**, 1165 (1976).

²A. J. Millis, Phys. Rev. B **48**, 7183 (1993).

³T. Moriya and T. Takimoto, J. Phys. Soc. Jpn. **64**, 960 (1995).

⁴G. R. Stewart, Rev. Mod. Phys. **73**, 797 (2001).

⁵C. Petrovic, P. G. Pagliuso, M. F. Hundley, R. Movshovich, J. L. Sarrao, J. D. Thompson, Z. Fisk, and P. Monthoux, J. Phys.: Condens. Matter **13**, L337 (2001).

⁶J. S. Kim, J. Alwood, G. R. Stewart, J. L. Sarrao, and J. D. Thompson, Phys. Rev. B **64**, 134524 (2001).

⁷V. A. Sidorov, M. Nicklas, P. G. Pagliuso, J. L. Sarrao, Y. Bang, A. V. Balatsky, and J. D. Thompson, Phys. Rev. Lett. **89**, 157004 (2002).

⁸J. Paglione, M. A. Tanatar, D. G. Hawthorn, E. Boaknin, R. W. Hill, F. Ronning, M. Sutherland, L. Taillefer, C. Petrovic, and P. C. Canfield, Phys. Rev. Lett. **91**, 246405 (2003).

⁹A. Bianchi, R. Movshovich, I. Vekhter, P. G. Pagliuso, J. L. Sarrao, Phys. Rev. Lett. **91**, 257001 (2003).

¹⁰A. Bianchi, R. Movshovich, N. Oeschler, P. Gegenwart, F. Steglich, J. D. Thompson, P. G. Pagliuso, and J. L. Sarrao, Phys. Rev. Lett. **89**, 137002 (2002).

¹¹F. Ronning, C. Capan, A. Bianchi, R. Movshovich, A. Lacerda, M. F. Hundley, J. D. Thompson, P. G. Pagliuso, and J. L. Sarrao, Phys. Rev. B **71**, 104528 (2005).

¹²E. D. Bauer, C. Capan, F. Ronning, R. Movshovich, J. D. Thompson, and J. L. Sarrao, Phys. Rev. Lett. **94**, 047001 (2005).

¹³G. Sparn, R. Borth, E. Lengyel, P. G. Pagliuso, J. L. Sarrao, F.

Steglich, and J. D. Thompson, Physica B **319**, 262 (2002).

¹⁴Y. Kohori, H. Saito, Y. Kobayashi, H. Taira, Y. Iwamoto, T. Kohara, T. Matsumoto, E. D. Bauer, M. B. Maple, and J. L. Sarrao, J. Magn. Magn. Mater. **272-276**, 189 (2004).

¹⁵H. Shishido, T. Ueda, S. Hashimoto, T. Kubo, R. Settai, H. Harima, and Y. Onuki, J. Phys.: Condens. Matter **15**, L499 (2003).

¹⁶L. Taillefer, F. Piquemal, and J. Flouquet, Physica C **153**, 451 (1988).

¹⁷J. D. Thompson and J.M. Lawrence, *Handbook of the Physics and Chemistry of the Rare Earths* (Elsevier, Amsterdam, 1994), Vol. 19, p. 383.

¹⁸N. D. Mathur, F. M. Grosche, S. R. Julian, I. R. Walker, D. M. Freye, R. K. W. Haselwimmer, and G. G. Lonzarich, Nature (London) **394**, 39 (1998).

¹⁹J. Custers, P. Gegenwart, H. Wilhelm, K. Neumaier, Y. Tokiwa, O. Trovarelli, C. Geibel, F. Steglich, C. Pepin, and P. Coleman, Nature (London) **424**, 524 (2003).

²⁰S. A. Grigera, R. S. Perry, A. J. Schofield, M. Chiao, S. R. Julian, G. G. Lonzarich, S. I. Ikeda, Y. Maeno, A. J. Millis, and A. P. Mackenzie, Science **294**, 329 (2001).

²¹H. Shishido, R. Settai, H. Harima, and Y. Onuki, J. Phys. Soc. Jpn. **74**, 1103 (2005).

²²S. M. Ramos, M. B. Fontes, A. D. Alverenga, E. Baggio-Saitovitch, P. G. Pagliuso, E. D. Bauer, J. D. Thompson, J. L. Sarrao, and M. A. Continentino, Physica B **359**, 398 (2005).

²³J. Paglione, M. A. Tanatar, D. G. Hawthorn, E. Boaknin, F. Ronning, R. W. Hill, M. Sutherland, L. Taillefer, C. Petrovic, and P. C. Canfield, cond-mat/0405157 (unpublished).